Absolute Configuration of Lippifoliane and Africanane Derivatives

Carlos M. Cerda-García-Rojas,*,† Angelina del C. Coronel,‡ Marina E. P. de Lampasona,‡ César A. N. Catalán,‡ and Pedro Joseph-Nathan†

Departamento de Química, Centro de Investigación y de Estudios Avanzados del Instituto Politécnico Nacional, Apartado 14-740, México, D. F., 07000 México, and Instituto de Química Orgánica, Facultad de Bioquímica, Química y Farmacia, Universidad Nacional de Tucumán, Ayacucho 471, S. M. de Tucumán, 4000 Argentina

Received January 3, 2005

The absolute configuration of naturally occurring lippifoliane derivatives isolated from the widely used plant *Lippia integrifolia* was assigned by analysis of the circular dichroism data in combination with density functional theory minimum energy molecular models of (1*S*,4*R*,6*S*,9*S*,10*R*)-lippifolian-1-ol-5-one (**1**), (4*R*,9*S*,10*R*)-lippifoli-1(6)-en-5-one (**2**), and (4*S*,9*S*,10*R*)-lippifoli-1(6)-en-4-ol-5-one (**3**) and application of the octant rule for saturated ketone **1** and the helicity rules for α,β-unsaturated ketones **2** and **3**. The results were reinforced by the anomalous dispersion effect observed in the X-ray diffraction analysis of (4*S*,9*S*,10*R*)-4,10,11-tribromo-10,11-*seco*-lippifoli-1(6)-en-5-one (**4**) prepared from **2**. The biogenetic relationships between lippifolianes **1**−**3** and africanane derivatives **7**−**9** and **13** isolated from the same species, together with chiroptical data for africananes isolated from the Hepaticae family, complete a stereochemical scenario in relation to the absolute configuration of africananes from *L. integrifolia*.

Lippifoliane derivatives constitute a representative group of secondary metabolites that possess the tricyclo[5.4.0.0^{2,4}]-undecane ring system. These substances have been isolated from *Lippia integrifolia* Hieron. (Verbenaceae),[1,2] a woody aromatic shrub native to central and northern Argentina that is widely used in a large number of commercial preparations as well as in traditional medicine as a diuretic, emmenagogue, stomachic, and nervine agent.[3,4] In the present work, we have applied theoretical and experimental methodologies to determine the absolute configuration of this group of sesquiterpenes employing lippifoliane derivatives **1**−**3** (Figure 1). The study includes a detailed description of the geometries and molecular conformations of these three compounds obtained by density functional theory molecular modeling,[5] a comparison between the calculated and observed ^{1}H NMR coupling constant data,[6] and the X-ray diffraction of **2**. The accurate description of the molecular structure allowed us to carry out a confident analysis of the circular dichroism data in terms of classical and recent reviews about the octant rule[7−11] for **1** and the helicity rules[11−14] for **2** and **3**. In addition, the anomalous dispersion effect observed in the X-ray analysis of tribromo derivative **4** provided straightforward information for the determination of the absolute configuration of lippifolianes and the biogenetically related africanane derivatives **7**−**9** and **13** also obtained from *L. integrifolia*.

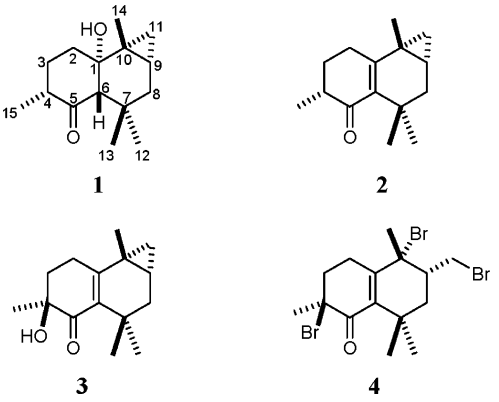

1 **2** **3** **4**

Figure 1. Lippifoliane derivatives **1**−**3** from *Lippia integrifolia* and 4,10,11-tribromo derivative **4**.

Results and Discussion

A conformational distribution for lippifoliane derivatives **1**−**3** was modeled by means of Monte Carlo random search[15] employing the Merck Molecular Force Field (MMFF) as implemented in the Spartan program. The minimum energy structures were selected according to their geometrical parameters and molecular mechanics relative energy within a range from 0 to 5 kcal/mol. The selected structures were geometry optimized by density functional theory calculations employing the B3LYP/6-31G* basis set. Table 1 lists the total energy, the conformer population, and the geometry of the more relevant minimum energy conformers of lippifoliane derivatives **1**−**3**. The percentage distribution for the conformers was estimated by taking into consideration the Boltzmann populations in relation to their DFT energy values as detailed in the Experimental Section,[16,17] while a quantitative description of the six-membered rings geometry of **1**−**3** was achieved by using the polar set of parameters proposed by Cremer and Pople.[18] These parameters were calculated with the RICON program,[19] using the DFT coordinates. As can be seen in Table 1, lippifoliane (**1**) may exist essentially in two conformations, **1a** and **1b**, in 89.7 and 10.2% (Figure 2), respectively, while the theoretical conformational analyses of **2** and **3** indicate the presence of three relevant conformers, which account for 96.8 and 99.9% of the conformational population, respectively (Figure 3). For compound **2**, the global minimum **2a** and the second minimum **2b** have the methyl group at C_4 in a quasi-equatorial orientation, while in the third minimum this group has an axial orientation. Conversely, in lippifoliane derivative **3**, the global minimum (**3a**) and the second minimum (**3b**) have a conformation in which the methyl

* To whom correspondence should be addressed. Tel: (+52-55)-5747-7112. Fax: (+52-55)-5747-7137. E-mail: ccerda@cinvestav.mx.
† Centro de Investigación y de Estudios Avanzados del Instituto Politécnico Nacional.
‡ Universidad Nacional de Tucumán.

10.1021/np050004n CCC: $30.25
Published on Web 03/24/2005

Table 1. Density Functional Theory (B3LYP/6-31G*) Energy, Conformational Population, and Conformational Parameters of Ring A (C_1−C_2−C_3−C_4−C_5−C_6) and Ring B (C_1−C_6−C_7−C_8−C_9−C_{10}) for the Main Minimum Energy Conformers of Lippifoliane Derivatives **1**−**3**

conformer	E_{DFT}[a]	population[b]	Q_A[c]	ϕ_A[d]	θ_A[d]	ring A conformation	Q_B[c]	ϕ_B[d]	θ_B[d]	ring B conformation
1a[e]	−736.466924	89.743	0.604	109.0	175.9	distorted chair	0.457	208.8	13.2	distorted half-chair
1b[e]	−736.464877	10.256	0.537	212.5	155.0	between half-chair and chair	0.722	133.8	98.6	between screw boat and boat
2a[f]	−660.049492	74.616	0.534	239.3	115.8	distorted envelope	0.469	95.4	70.6	between screw boat and boat
2b[f]	−660.048248	20.000	0.516	273.7	130.0	distorted half-chair	0.278	290.8	124.0	between envelope and screw boat
2c[f]	−660.046142	2.147	0.465	97.8	41.9	between half-chair and envelope	0.476	91.4	69.5	screw boat
3a[g]	−735.265226	75.973	0.466	99.0	42.4	between half-chair and envelope	0.475	90.7	69.3	screw boat
3b[g]	−735.263746	15.843	0.491	85.2	56.8	distorted half-chair	0.305	301.5	115.0	distorted envelope
3c[g]	−735.263115	8.120	0.548	223.1	111.0	between envelope and twist	0.472	92.6	69.8	distorted screw boat

[a] Quantum mechanics energy in hartrees. [b] Percentage of population. [c] Total puckering amplitude in Å. [d] Phase angles in deg. [e] Only the lowest energy conformer arising from rotation of the C_1−OH bond is listed. The third most populated conformer (0.0006%) has E_{DFT} = −736.455594 hartrees. [f] The fourth most populated conformer (1.561%) has E_T = −660.045841 hartrees. [g] Only the lowest energy conformer arising from rotation of the C_4−OH bond is listed. The fourth most populated conformer (0.063%) has E_T = −735.258532 hartrees.

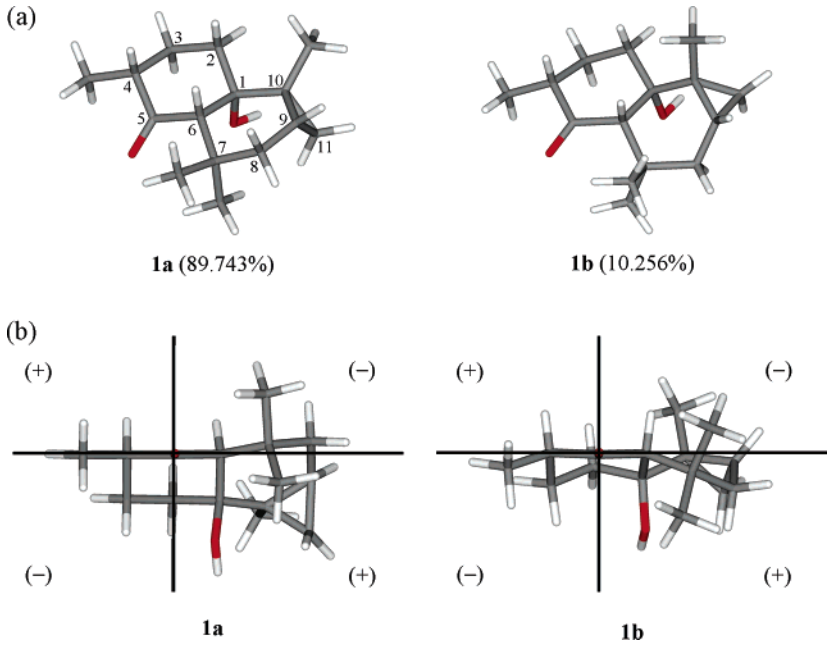

Figure 2. (a) Global and the second minimum energy DFT conformations of lippifoliane derivative **1** and (b) application of the octant rule.

group at C_4 has an axial orientation, while the third minimum **3c** has the methyl group in a quasi-equatorial orientation.

Experimental evidence to validate the theoretical conformations was obtained by comparing the calculated and observed ^{1}H−^{1}H vicinal coupling constants, which can be found in Table 2. Conversions from dihedral angles to vicinal coupling constants ($^3J_{H-H}$) for each conformer were done using the Altona equation.[20,21] The good correlation between the vicinal coupling constants calculated from the quantum mechanics dihedral angles and those observed for **1**−**3** supported the conformation of lippifoliane derivatives in solution. The major conformations of **3** with the axial orientation of the methyl group at C_4 (**3a** and **3b**) were evidenced by the presence of a *W*-type coupling constant between Me_{15} and $H_{3\beta}$ ($J_{3\beta,15}$ = 0.5 Hz) as well as the NOE effect (11%) measured for $H_{2\beta}$ (ddd, $J_{2\alpha,2\beta}$ = 18.7, $J_{2\beta,3\alpha}$ = 1.7, $J_{2\beta,3\beta}$ = 6.3 Hz) upon irradiation of the methyl group at C_{10}.[2] These conformations gain stability from the intramolecular hydrogen bond between the hydrogen of the equatorial hydroxyl group at C_4 and the carbonyl group at C_5 (Figure 3). The vicinal coupling constants of **1**−**3** were measured in $CDCl_3$, C_6D_6, and/or CD_3OD without observing substantial variations, except for $J_{2\alpha,3\beta}$ (11.4 Hz in $CDCl_3$ and 10.6 Hz in CD_3OD) and $J_{2\beta,3\alpha}$ (1.7 Hz in $CDCl_3$ and 3.0 Hz in CD_3OD) in **3**, which may reflect a slight modification in the conformation of the cyclohexenone moiety, due to the influence on the C_4−O_4−H--O_5=C_5 hydrogen bond when going from an aprotic to a protic solvent. Additionally, the ^{1}H and ^{13}C NMR assignments of **1**−**3** were confirmed by 2D NMR experiments.[2,22]

Crystallization of lippifoli-1(6)-en-5-one (**2**) afforded good quality prisms for the X-ray diffraction analysis of this natural product, whose structure is depicted in Figure 4. This study corroborated the relative stereochemistry of **2** originally proposed on the basis of NMR data and chemical correlation with integrifolian-1,5-dione (**12**).[1] Also, it is relevant to point out that the X-ray conformation of **2** (Figure 4) was essentially the same as that obtained for the density functional theory global minimum of this compound, represented by the B3LYP/6-31G* molecular model **2a** in Figure 3.

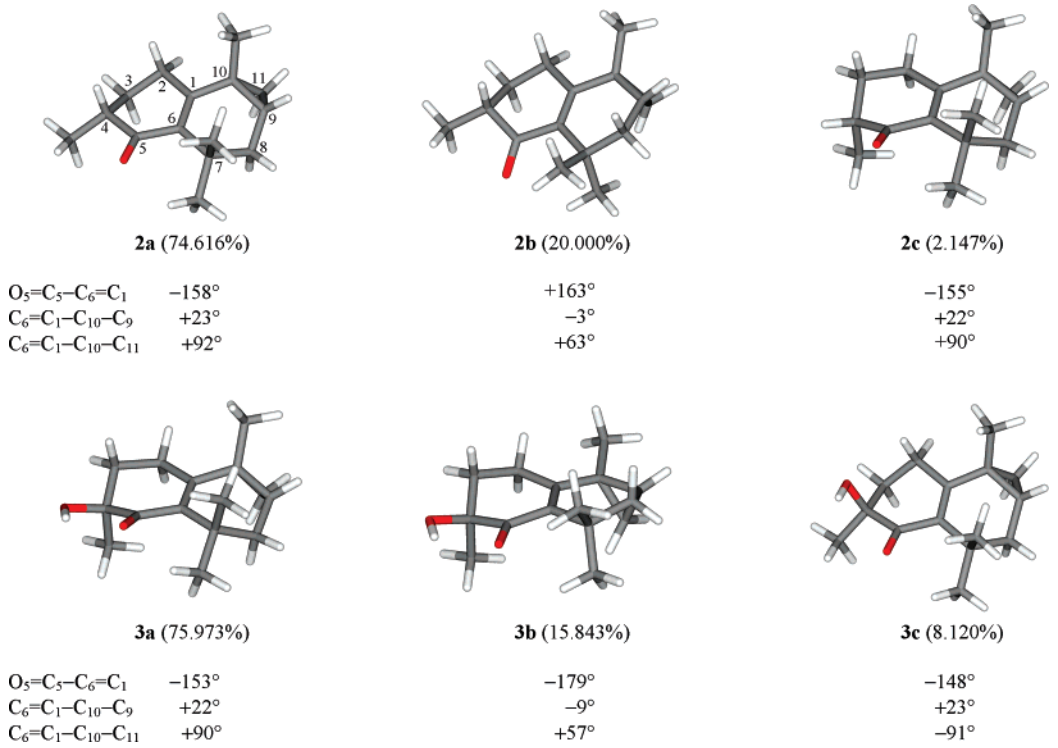

Figure 3. The three most relevant DFT conformations of lippifoliane derivatives **2** and **3**.

Table 2. Calculated and Observed $^1H-^1H$ Vicinal Coupling Constants for Lippifoliane Derivatives **1**–**3**

	1		**2**		**3**	
J	calculated	observed[a]	calculated	observed[a]	calculated	observed[a]
2α,3α	3.5	*b*	4.0	4.8	5.8	5.7
2α,3*β*	3.0	*b*	2.6	3.3	11.5	11.4
2*β*,3α	13.2	11.6	12.3	11.4	2.3	1.7
2*β*,3*β*	3.8	5.5	4.2	4.8	5.3	6.3
3α,4	12.3	13.0	11.7	12.8		
3*β*,4	3.4	5.5	3.2	4.8		
8α,9	2.2	2.0	5.3	5.8	5.6	5.8
8*β*,9	6.2	5.0	8.4	8.2	8.9	8.3

[a] In $CDCl_3$. [b] Not measured due to signal overlapping.

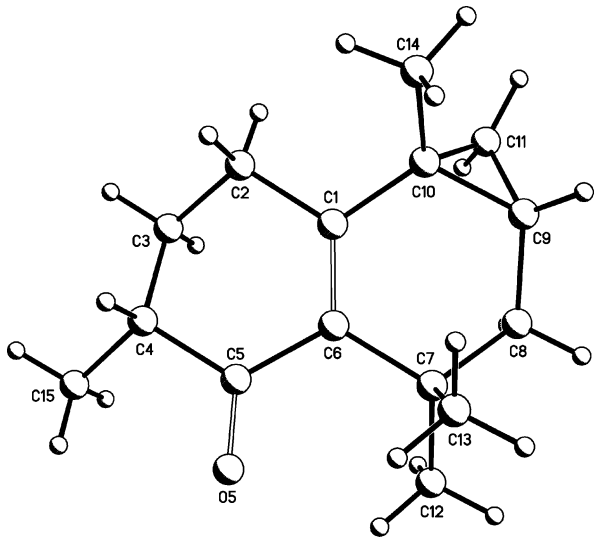

Figure 4. X-ray diffraction structure of (4*R*,9*S*,10*R*)-lippifoli-1(6)-en-5-one (**2**).

The DFT molecular models allowed us to have a clear picture of the relative stereochemistry and conformational behavior making possible the determination of the absolute configuration of lippifoliane derivatives in terms of the octant rule[7–11] for **1** and the helicity rules[11–14] for **2** and **3**. As can be seen for compound **1** (Figure 2), the major part of the molecular volume of the main conformer (**1a**) is located in positive octants. The hydroxyl group at C_1, the cyclopropyl moiety, and the methyl group at C_{10} are located in a positive octant, while the methyl group at C_4 remains in an equatorial position without a relevant influence on the Cotton effect, as well as the *gem*-dimethyl group because one of its methyl groups lies on a negative octant and the other methyl group lies in a positive octant. In the next minimum energy conformation (**1b**), the hydroxyl group at C_1, the cyclopropyl moiety, and one of the methyl groups at C_7 are located in a positive octant, while the other methyl group at C_7 and the methyl group at C_{10} lie on a negative octant. The methyl group at C_4 remains in an equatorial position without a relevant influence on the Cotton effect. The third minimum energy structure, which contributes with only 0.0006% of the conformational population, can be neglected. A quantitative evaluation of the approximate molecular volume located in the positive and in the negative octants for structures **1a** and **1b** appears in Table 3. According to these results and the absolute configuration shown in Figure 2, the expected sign of the Cotton effect for the $n \rightarrow \pi^*$ ketone transition in the circular dichroism curve is positive, in agreement with the sign of the observed molecular ellipticity $[\theta]_{295} = +263$ (Figure 5).

Table 3. Molecular Volume in Å^3 of Conformations **1a** and **1b**

molecular volume	1a	1b
total	328	325
in neutral space	119	70
in positive octants	144	149
in negative octants	65	106
difference (positive − negative)	+79	+43

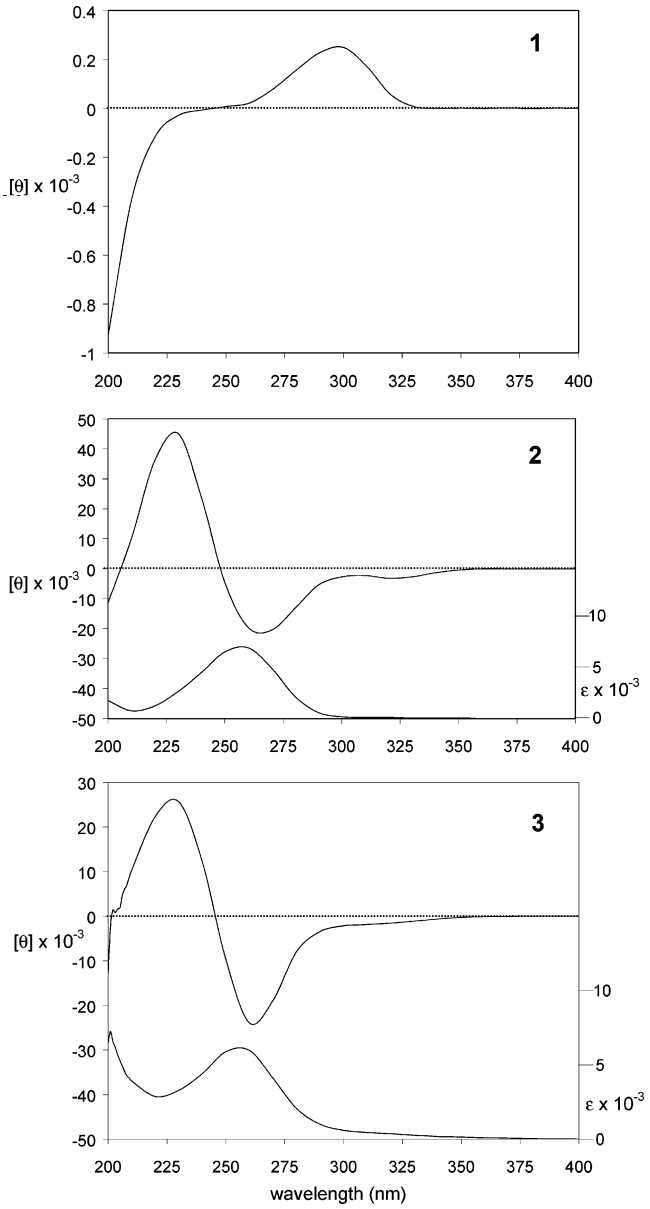

Figure 5. Circular dichroism of lippifoliane **1** (top) and circular dichroism and UV spectra of lippifolianes **2** (middle) and **3** (bottom).

On the basis of biogenetic considerations, the absolute configuration of lippifolianes **1**−**3** should be the same (Figure 1). In fact, the similarity between the circular dichroism curves of both α,β-unsaturated ketones **2** and **3** (Figure 5) indicated that the two substances have the same absolute configuration. The molecular modeling studies of **2** and **3** revealed that the main conformations of both lippifolienones possess inherently dissymmetric chromophores, since the C=C−C=O moieties are not planar. According to the enone helicity rules,[11−14] the rotatory strength of such chromophores can assume values approximately 100 times greater than inherently symmetric but dissymmetrically perturbed chromophores. The circular dichroism curve of lippifolienone **2** clearly showed the intense *K* band ($\pi \rightarrow \pi^*$ transition) at 266 nm with a negative value of $[\theta]_{266} = -22\,700$ (Figure 5). In agreement with the helicity rules for α,β-unsaturated ketones, this value corresponds to a negative chirality,[14] as shown in Figure 3, where the $O_5{=}C_5{-}C_6{=}C_1$ dihedral angles Φ of the global minimum **2a** and the third minimum **2c** are negative with values of −158° and −155°, respectively. Both conformers contribute more than 75% to the total conformational population. The second minimum (**2b**) displayed a positive dihedral angle (Φ = +163°), but its contribution is only 20%. In the case of lippifolienone **3**, this angle is negative in the global, the second, and the third minima, having values of −153°, −179°, and −148°, respectively. Therefore, structure **3** (Figure 3) also possesses the chirality associated with the negative value for an even more intense *K* band with a molecular ellipticity of $[\theta]_{263} = -25\,900$ (Figure 5).

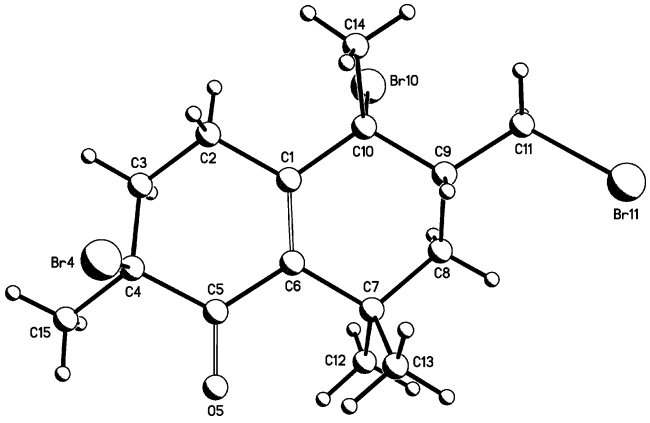

Figure 6. X-ray diffraction structure of (4*S*,9*S*,10*R*)-4,10,11-tribromo-10,11-*seco*-lippifoli-1(6)-en-5-one (**4**).

Confirmatory proof for the absolute configuration of lippifoliane derivatives from *L. integrifolia* was obtained in view of the anomalous dispersion factor obtained by refinement of X-ray diffraction data for (4*S*,9*S*,10*R*)-4,10,-11-tribromo-10,11-*seco*-lippifoli-1(6)-en-5-one (**4**) and its enantiomer. The correct enantiomer (Figure 6) converged to an $R_F = 2.8\%$, while the antipodal structure showed a higher value ($R_F = 3.2\%$). In agreement with this finding, the absolute structure parameter, the Flack parameter,[23,24] displayed a value near zero (0.098 ± 0.051) for the correct enantiomer, while data refinement using the antipodal structure showed 0.776 ± 0.057. Compound **4** was prepared by treatment of (4*R*,9*S*,10*R*)-lippifoli-1(6)-en-5-one (**2**) with bromine in carbon tetrachloride. In this reaction, addition of bromine to the cyclopropane ring proceeds with ring opening at the $C_{10}{-}C_{11}$ bond, but the chiral center at C_9 remains intact and, therefore, it can be used as the center of reference to define the absolute configuration of **2** and its biogenetically related compounds.

Once the absolute configuration was unambiguously determined, it is pertinent to discuss the potential contribution of the vinylogous cyclopropyl group of **2** and **3** to the Cotton effect. It is known that in α,β-cyclopropyl ketones there is a maximum orbital overlapping when the plane of the three-membered ring lies perpendicular to the plane of the R−C=O group and parallel to the π-orbital of the carbonyl group.[11] If this concept is extended to γ-cyclopropyl-α,β-unsaturated ketones, the arrangement of maximum overlap can be represented by Figure 7a, where the $O{=}C{-}C_\alpha{=}C_\beta$ dihedral angle is 180° and the $C_\alpha{=}C_\beta{-}C_\gamma{-}C_\delta$ and $C_\alpha{=}C_\beta{-}C_\gamma{-}C_{\delta'}$ dihedral angles are +145° and −145°, respectively, averaging 180°. Figure 7b shows a molecular fragment that nearly represents the chro-

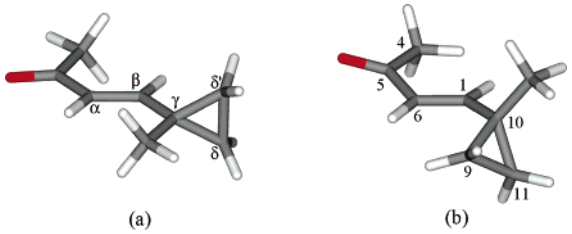

Figure 7. (a) γ-Cyclopropyl-α,β-unsaturated ketone fragment in the maximum π-orbital overlap conformation and (b) the fragment as found in lippifolienones **2** and **3**.

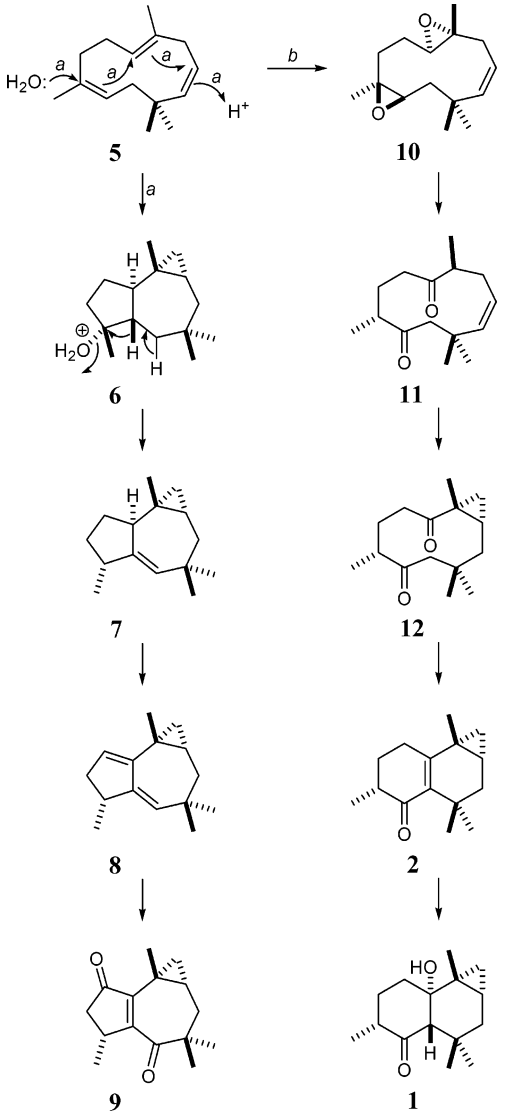

Figure 8. Proposed biogenetic pathway for some representative metabolites of *Lippia integrifolia*.

mophore of the main conformations **2a** and **3a** (Figure 3), where the $C_6{=}C_1{-}C_{10}{-}C_{11}$ and $C_6{=}C_1{-}C_{10}{-}C_9$ dihedral angles are ca. +91° and +23°, respectively, averaging +57°. The sign of this value is opposite that found for the $O_5{=}C_5{-}C_6{=}C_1$ dihedral angles ($\Phi = -158°$ in **2a** and $\Phi = -153°$ in **3a**). Therefore, an opposite contribution of the cyclopropyl moiety to the Cotton effect of **2** and **3** may be expected.

It is clear that the dominant effect for the helicity rule must be that arising from the $O_5{=}C_5{-}C_6{=}C_1$ fragment since the UV $\pi \rightarrow \pi^*$ maximum for both substances can be found at 256 nm, which is only 7 nm higher than the calculated value[13] for a molecule without the cyclopropyl

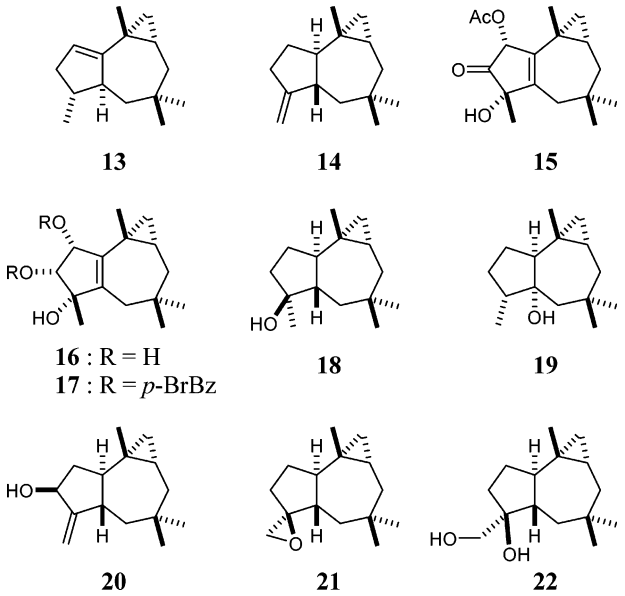

Figure 9. Africanane derivatives **13** and **14** from the liverwort *Pellia epiphylla*, **15** and **16** from the liverwort *Porella caespitans*, **18** and **19** from the fungus *Leptographium lundbergii*, and **20**−**22** from the soft coral *Sinularia dissecta*. Compound **13** was also isolated from *Lippia integrifolia*.

moiety. It has been stated that the relative orientation of a cyclopropane ring plays a crucial role in determining whether this group behaves as an inherently dissymmetric chromophore, or if it contributes as an allylic substituent.[12,13] The latter situation may be the case here. However, this contribution may be partially canceled by the contribution of the C_{14} methyl group. To the best of our knowledge, **2** and **3** are the first examples of circular dichroism data of γ-cyclopropyl-α,β-unsaturated ketones, a fact that further extends the applications of circular dichroism methods.

The biogenesis of lippifoliane derivatives (Figure 8) can be considered as structurally interrelated with the biogenesis of africanane derivatives **7**−**9** and **13** (Figures 8 and 9), which were also isolated from *L. integrifolia*.[4,25] It is relevant to mention that besides **1**−**3**, **7**−**9**, and **13**, this plant affords (*S*)-(+)-*trans*-nerolidol,[4] humulene (**5**),[26] the bicyclohumulenedione **11**,[27] and integrifolian-1,5-dione (**12**),[1] which support the proposed biogenetic pathway. On the basis of the lippifoliane−africanane relationship, we can conclude that the absolute configuration of africanane derivatives from the genus *Lippia* is as represented in Figure 8. Compounds **6** and **10** have not been isolated yet from *L. integrifolia*, but are known natural products.[28,29]

Africanane derivatives have been isolated from diverse natural sources (Figure 9) including **13** and **14** from the liverwort *Pellia epiphylla*,[30] **15** and **16** from the liverwort *Porella caespitans*,[31] **6**, **18**, and **19** from the ascomycete fungus *Leptographium lundbergii*,[28] and **20**−**22** from the soft coral *Sinularia dissecta*.[32] The absolute configuration of **13** from *L. integrifolia* (Verbenaceae) is the same as that of **13** isolated from *P. epiphylla* (Hepaticae) as deduced from identical GC retention times on several modified cyclodextrin stationary phases and optical rotation values.[25] Furthermore, the absolute configuration of the chiral centers at C-9 and C-10 of **15** and **16**, isolated from *P. caespitans* (Hepaticae), is the same as that of **1**−**3**, **7**−**9**, and **13** from *L. integrifolia*. The absolute configuration of **15** and **16** was secured by the exciton chirality method[33,34] using the 2,3-di-*p*-bromobenzoyl derivative **17** and its C-3 epimer.[31] These facts complete a stereochemical scenario that seems to point out that africanane derivatives from

plants and liverworts could have a similar biogenetic origin. Finally, the absolute configuration of **6**, **18**, and **19** isolated from the fungus *L. lundbergii*,[28] and of **20**−**22** isolated from the marine organism *S. dissecta* (Alcyoniidae),[32] remains unknown. Therefore, it will be desirable to further explore whether the absolute configuration of africanane derivatives varies according to their origin in nature.

In summary, the absolute configuration of lippifioliane derivatives isolated from the widely used plant *L. integrifolia* has been established as shown in Figure 1. The accurate description of the molecular geometry achieved by DFT molecular modeling and NMR spectroscopy has allowed us to accomplish a confident analysis of the circular dichroism data in terms of the octant rule[7−11] for **1** and the helicity rules[11−14] for **2** and **3**. The helicity rules are valid for the γ-cyclopropyl-α,β-unsaturated ketones present in lippifolianes **2** and **3**, as it was fully confirmed from the anomalous dispersion effect shown by the X-ray data of tribromo derivative **4**. The biogenetic relationships among the natural products isolated from *L. integrifolia* (Figure 8) have also allowed the assignment of the absolute configuration of africanane derivatives **7**−**9** and **13**.

Experimental Section

General Experimental Procedures. Circular dichroism measurements in MeOH were determined on a JASCO J-720 spectropolarimeter. NMR spectra were measured on a Varian Mercury 300 spectrometer. The residual solvent peak was used to reference the spectra. Compounds **1**−**3** were obtained from *Lippia integrifolia* (Verbenaceae) as previously described.[1,2]

Computational Details. The molecular modeling calculations started with a systematic conformational search for both six-membered rings of lippifoliane derivatives **1**−**3**. This procedure was carried out with the aid of Dreiding models considering torsion angle rotations of ca. 20° in those bonds, which allowed such movements. All rotamer species derived from the hydroxyl group rotation of **1** and **3** were examined. Geometry optimizations were carried out using the MMFF94 force-field calculations.[35] The E_{MMFF94} values were used as the convergence criterion, and a further search with the Monte Carlo protocol[15,36] was carried out considering an energy cutoff of 10 kcal/mol above the global minimum. Within this range, sets of 15, 4, and 5 different conformations were found and geometry was analyzed for **1**, **2**, and **3**, respectively. All conformers were submitted to density functional theory calculations (DFT/B3LYP/6-31G*)[37,38] without any restriction of the O−H bond rotation. Conformers that accounted for at least 95% of the total population of each compound were included in Table 1. The MMFF94 force-field calculations, the Monte Carlo random searching, and the density functional theory B3LYP/6-31G* quantum calculations were achieved with the Spartan′02 software from Wavefunction, Inc. (Irvine, CA).[38]

A cyclic equilibrium at 298 K among all the calculated conformers for compounds **1**−**3** was modeled. For example, the case of an equilibrium among three conformers was treated by considering $k_{1,2} = n_2/n_1$, $k_{2,3} = n_3/n_2$, $k_{3,1} = n_1/n_3$, and $n_1 + n_2 + n_3 = 1$.[16,39] Taking into account the Boltzmann equation $n_i = e^{-\Delta E(i)/kT}/\sum_j e^{-\Delta E(j)/kT}$ where ΔE is the DFT energy difference between pairs of conformers, equations $n_1 = n_2 e^{-(E_2-E_1/kT)}$, $n_3 = n_2 e^{-(E_2-E_3/kT)}$, and $n_2 = 1 - n_1 - n_3$ were employed to calculate the conformational populations.

Conversions of dihedral angles into vicinal coupling constants ($^3J_{H-H}$) for each conformer were done using the Altona equation.[20,21] The population-weighted average coupling constant for each H−C−C−H dihedral fragment was calculated using the equation $^3J_{calc} = n_1J_1 + n_2J_2 + ... + \sum n_iJ_i$.

Approximate molecular volumes were calculated by selecting those atoms whose center of mass lie in a defined octant, deleting the nonselected atoms, and calculating the molecular volumes of the remaining fragment. This was achieved by using the graphical interface provided by the Spartan software. Atoms whose centers lie in or very near to the *x*, *y*, or *z* axes were not taken into account.

(4*S*,9*S*,10*R*)-4,10,11-Tribromo-10,11-*seco*-lippifoli-1(6)-en-5-one (4). A solution of lippifoli-1(6)-en-5-one **2** (64 mg) in CCl_4 (5 mL) was cooled to 0 °C and treated dropwise with a solution of Br_2 (25 μL) in CCl_4 (0.5 mL). The reaction mixture was stirred at 0 °C for 2 h, treated with a saturated aqueous solution of $NaHSO_3$ (25 mL), and extracted with $CHCl_3$ (2 × 50 mL). The organic layer was washed with the $NaHSO_3$ solution (5 × 25 mL), H_2O (2 × 25 mL), a saturated solution of $NaHCO_3$ (2 × 25 mL), and H_2O (2 × 25 mL), dried over anhydrous Na_2SO_4, and evaporated. The product was crystallized from CH_2Cl_2−pentane to afford **4** (41 mg, 30%) as colorless prisms: mp 139−141 °C; $[\alpha]_{589}$ +5°, $[\alpha]_{578}$ +3°, $[\alpha]_{546}$ −5°, $[\alpha]_{436}$ −172° (*c* 2.23, $CHCl_3$); IR ν_{max} ($CHCl_3$) 1672 (C=O), 1590 cm^{-1} (C=C); UV (EtOH) λ_{max} (log ϵ) 265 nm (4.00); ^1H NMR ($CDCl_3$, 300 MHz) δ 3.77 (1H, dd, $J_{9,11'} = 2.4$, $J_{11,11'} = 10.1$ Hz, H-11′), 3.23 (1H, dd, $J_{9,11} = 9.0$, $J_{11,11'} = 10.1$ Hz, H-11), 2.82 (1H, ddd, $J_{2\alpha,2\beta} = 18.1$, $J_{2\alpha,3\alpha} = 4.7$, $J_{2\alpha,3\beta} = 2.7$ Hz, H-2α), 2.67 (1H, ddd, $J_{2\alpha,2\beta} = 18.1$, $J_{2\beta,3\alpha} = 10.7$, $J_{2\beta,3\beta} = 4.1$ Hz, H-2β), 2.35 (1H, ddd, $J_{2\alpha,3\beta} = 2.7$, $J_{2\beta,3\beta} = 4.1$, $J_{3\alpha,3\beta} = 14.8$ Hz, H-3β), 1.95 (3H, s, Me-15), 1.90 (1H, dd, $J_{8\alpha,8\beta} = 12.6$, $J_{8\beta,9} = 2.2$ Hz, H-8β), 1.88 (3H, s, Me-14), 1.87 (1H, ddd, $J_{2\alpha,3\alpha} = 4.7$, $J_{2\beta,3\alpha} = 10.7$, $J_{3\alpha,3\beta} = 14.8$ Hz, H-3α), 1.82 (1H, dddd, $J_{8\alpha,9} = 12.6$, $J_{8\beta,9} = 2.2$, $J_{9,11} = 9.0$, $J_{9,11'} = 2.4$ Hz, H-9), 1.69 (1H, dd, $J_{8\alpha,8\beta} = 12.6$, $J_{8\alpha,9} = 12.6$ Hz, H-8α), 1.28 (3H, s, Me-12), 1.24 (3H, s, Me-13); ^{13}C NMR ($CDCl_3$, 75.4 MHz) δ 191.7 (C-5), 154.5 (C-1), 135.6 (C-6), 71.3 (C-10), 63.9 (C-4), 45.6 (C-9), 41.7 (C-8), 38.4 (C-3), 35.6 (C-11), 34.3 (C-7), 29.5 (C-12), 28.7 (C-15), 28.4 (C-14), 25.7 (C-12), 25.6 (C-2); EIMS *m/z* 457 $[M]^+$ (4), 379 (33), 377 (66), 375 (34), 335 (10), 299 (9), 298 (49), 297 (79), 296 (57), 295 (73), 294 (10), 218 (16), 227 (100), 216 (71), 215 (77), 203 (81), 201 (83), 173 (99).

X-ray Diffraction Analysis of 2 and 4. The X-ray data were measured on a Bruker-Nonius CAD4 diffractometer equipped with Cu Kα radiation (λ = 1.54178 Å). The structures were solved by direct methods using SHELXS97.[40] For the structural refinement, the non-hydrogen atoms were treated anisotropically, and the hydrogen atoms, included in the structure factor calculation, were refined isotropically.

Single crystals of **2** (mp of 35−37 °C) were grown by slow crystallization of the pure compound (ca. 1 g) at −20 °C without using any solvent. A crystal of size 0.26 × 0.22 × 0.20 mm^3 was placed in a capillary glass and subjected to the X-ray diffraction analysis. It was monoclinic, space group $P2_1$, with $a = 8.765(1)$ Å, $b = 8.783(5)$ Å, $c = 9.004(2)$ Å, $\beta = 106.55(1)°$, cell volume = 664.4(4) $Å^3$, $\rho_{calcd} = 1.09$ g/cm^3 for $Z = 2$, MW = 218.32, and $F(000)e^- = 240$. A total of 991 reflections were collected within a θ range of 5.12−54.90° for $0 \le h \le 9$, $0 \le k \le 9$, $-9 \le l \le 9$. The unique reflections were 895, and final discrepancy indices were $R_F = 4.2\%$ and $R_W = 12.1\%$ refining 146 parameters.

Single crystals of **4** were grown by crystallization from CH_2Cl_2−pentane. The size of the crystal used was 0.32 × 0.30 × 0.20 mm^3. It was orthorhombic, space group $P2_12_12_1$, with $a = 9.365(3)$ Å, $b = 10.104(8)$ Å, $c = 18.154(4)$ Å, cell volume = 1717.9(7) $Å^3$, $\rho_{calcd} = 1.77$ g/cm^3 for $Z = 4$, MW = 457.04, and $F(000)e^- = 950$. A total of 1310 reflections were collected within a θ range of 4.87−54.95° for $0 \le h \le 9$, $0 \le k \le 10$, $0 \le l \le 19$. The unique reflections were 1262, and final discrepancy indices, refining 172 parameters, were $R_F = 2.8\%$ and $R_W = 7.5\%$. The enantiomeric structure of **4** showed $R_F = 3.2\%$ and $R_W = 8.4\%$. The Flack parameter for **4** was near zero (0.098 ± 0.051), while its antipodal structure showed a Flack parameter of 0.776 ± 0.057. No attempt was made to ascertain the absolute configuration of **2**. Crystallographic data for both structures have been deposited with the Cambridge Crystallographic Data Centre. The CCDC deposition number for **2** is 264348 and that for **4** is 264349. Copies of the data can be obtained, free of charge, on application to the Director, CCDC, 12 Union Road, Cambridge CB2 1EZ, UK. Fax: +44-(0)1223-336033 or e-mail: deposit@ccdc.cam.ac.uk.

Acknowledgment. The authors thank CONACYT-Mexico (G-32631-N) for financial support and M. del Rocío Patiño

Maya, Instituto de Química, Universidad Nacional Autónoma de México, for recording the circular dichroism spectra. Work in Tucumán was supported by grants from Consejo Nacional de Investigaciones Científicas y Técnicas de Argentina (CONICET) and Consejo de Investigaciones de la Universidad Nacional de Tucumán (CIUNT). Stimulating support from CYTED, Spain, is also acknowledged.

Supporting Information Available: Atomic coordinates, bond distances, and bond angles for compounds **2** and **4** are listed in S1−S7. This material is available free of charge via the Internet at http://pubs.acs.org.

References and Notes

(1) Catalán, C. A. N.; de Fenik, I. J. S.; Dartayet, G. H.; Gros, E. G. *Phytochemistry* **1991**, *30*, 1323−1326.
(2) Catalán, C. A. N.; de Lampasona, M. E. P.; de Fenik, I. J. S.; Cerda-García-Rojas, C. M.; Mora-Pérez, Y.; Joseph-Nathan, P. *J. Nat. Prod.* **1994**, *57*, 206−210.
(3) Toursarkissian, M. *Plantas Medicinales de la Argentina*; Hemisferio Sur: Buenos Aires, 1980; p 135.
(4) Catalán, C. A. N.; de Lampasona, M. E. P.; Cerda-García-Rojas, C. M.; Joseph-Nathan, P. *J. Nat. Prod.* **1995**, *58*, 1713−1717.
(5) Perdew, J. P. *Phys. Rev. B* **1986**, *33*, 8822−8824.
(6) Flores-Sandoval, C. A.; Cerda-García-Rojas, C. M.; Joseph-Nathan, P. *Magn. Reson. Chem.* **2001**, *39*, 173−178.
(7) Kirk, D. N.; Klyne, W. *J. Chem. Soc., Perkin Trans. 1* **1974**, 1076−1103.
(8) Kirk, D. N. *Tetrahedron* **1986**, *42*, 777−818.
(9) Legrand, M.; Rougier, M. J. In *Application of the Optical Activity to Stereochemical Determinations*; Kagan, H. B., Ed.; Stereochemistry Fundamental and Methods, Vol. 2, Determination of Configurations by Dipole Moments, CD or ORD; Georg Thieme Publishers: Stuttgart, 1977; pp 105−112.
(10) Lightner, D. A. In *Circular Dichroism-Principles and Applications*; Berova, N.; Nakanishi, K.; Woody, R. W., Eds.; Wiley-VCH: NewYork, 2000; pp 261−303.
(11) Lightner, D. A.; Gurst, J. E. *Organic Conformational Analysis and Stereochemistry from Circular Dichroism Spectroscopy*; Wiley-VCH: New York, 2000; Chapters 4, 7, and 11.
(12) Gawronski, J. *Tetrahedron* **1982**, *38*, 3−26.
(13) Gawronski, J. In *The Chemistry of Enones*; Patai, S., Rappoport, Z., Eds.; John Wiley and Sons: New York, 1989; pp 55−105.
(14) Snatzke, G. *Angew. Chem., Int. Ed. Engl.* **1968**, *7*, 14−25.
(15) Höltje, H. D.; Folkerts, G. In *Molecular Modeling. Basic Principles and Applications*; Mannhold, R.; Kubinyi, H.; Timmerman, H., Eds.; Methods and Principles in Medicinal Chemistry; VCH: Weinheim, 1996; Vol. 5, p 29.
(16) Arnó, M.; Marín, M. L.; Zaragozá, R. J. *Magn. Reson. Chem.* **1998**, *36*, 579−586.
(17) Pereda-Miranda, R.; Fragoso-Serrano, M.; Cerda-García-Rojas, C. M. *Tetrahedron* **2001**, *57*, 43−57.
(18) Cremer, D.; Pople, J. A. *J. Am. Chem. Soc.* **1975**, *97*, 1354−1358.
(19) Zotov, A.; Palyulin, V.; Zefirov, N. *RICON Program Version 5.05*; Moscow State University: Moscow, Rusia, 1994.
(20) Haasnoot, C. A. G.; de Leeuw, F. A. A. M.; Altona, C. *Tetrahedron* **1980**, *36*, 2783−2792.
(21) Cerda-García-Rojas, C. M.; Zepeda, L. G.; Joseph-Nathan, P. *Tetrahedron Comput. Methodol.* **1990**, *3*, 113−118.
(22) Catalán, C. A. N.; de Fenik, I. J. S.; Cerda-García-Rojas, C. M.; Mora-Pérez, Y.; Joseph-Nathan, P. *Spectroscopy* **1993**, *11*, 1−8.
(23) Flack, H. D. *Acta Crystallogr., Sect. A* **1983**, *39*, 876−881.
(24) Bernardinelli, G.; Flack, H. D. *Acta Crystallogr., Sect. A* **1985**, *41*, 500−511.
(25) Fricke, C.; Hardt, I. H.; König, W. A.; Joulain, D.; Zygadlo, J. A.; Guzmán, C. A. *J. Nat. Prod.* **1999**, *62*, 694−696.
(26) de Lampasona, M. E. P.; de Fenik, I. J. S.; Catalán, C. A. N.; Dartayet, G. H.; Gros, E. G.; Cerda-García-Rojas, C. M.; Mora-Pérez, Y.; Joseph-Nathan, P. *Acta Hortic.* **1999**, *500*, 81−88.
(27) Catalán, C. A. N.; de Lampasona, M. E. P.; de Fenik, I. J. S.; Cerda-García-Rojas, C. M.; Joseph-Nathan, P. *J. Nat. Prod.* **1993**, *56*, 381−385.
(28) Abraham, W. R.; Ernst, L.; Witte, L.; Hanssen, H. P.; Sprecher, E. *Tetrahedron* **1986**, *42*, 4475−4480.
(29) Ramaswami, S. K.; Bhattacharyya, S. C. *Tetrahedron* **1962**, *18*, 575−579.
(30) Cullmann, F.; Becker, H. *Phytochemistry* **1998**, *47*, 237−245.
(31) Toyota, M.; Nagashima, F.; Shima, K.; Asakawa, Y. *Phytochemistry* **1992**, *31*, 183−189.
(32) Ramesh, P.; Reddy, N. S.; Rao, T. P.; Venkateswarlu, Y. *J. Nat. Prod.* **1999**, *62*, 1019−1021.
(33) Harada, N.; Nakanishi, K. *Acct. Chem. Res.* **1972**, *5*, 257−263.
(34) Lin, Y. Y.; Risk, M.; Ray, S. M.; Van Engen, D.; Clardy, J.; Golik, J.; James, J. C.; Nakanishi, K. *J. Am. Chem. Soc.* **1981**, *103*, 6773−6775.
(35) (a) Halgren, T. *J. Comput. Chem.* **1996**, *17*, 490−519. (b) Halgren, T. *J. Comput. Chem.* **1996**, *17*, 520−552. (c) Halgren, T. *J. Comput. Chem.* **1996**, *17*, 553−586. (d) Halgren, T.; Nachbar, R. B. *J. Comput. Chem.* **1996**, *17*, 587−615. (e) Halgren, T. *J. Comput. Chem.* **1996**, *17*, 616−641.
(36) Chang, G.; Guida, W. C.; Still, W. C. *J. Am. Chem. Soc.* **1989**, *111*, 4379−4386.
(37) Hehre, W. J.; Radom, L.; Schleyer, P. V. R.; Pople, J. A. *Ab Initio Molecular Orbital Theory*; Wiley: New York, 1986.
(38) Kong, J.; White, C. A.; Krylov, A. I.; Sherrill, C. D.; Adamson, R. D.; Furlani, T. R.; Lee, M. S.; Lee, A. M.; Gwaltney, S. R.; Adams, T. R.; Ochsenfeld, C.; Gilbert, A. T. B.; Kedziora, G. S.; Rassolov, V. A.; Maurice, D. R.; Nair, N.; Shao, Y.; Besley, N. A.; Maslen, P. E.; Dombroski, J. P.; Daschel, H.; Zhang, W.; Korambath, P. P.; Baker, J.; Byrd, E. F. C.; Van Voorhis, T.; Oumi, M.; Hirata, S.; Hsu, C.-P.; Ishikawa, N.; Florian, J.; Warshel, A.; Johnson, B. G.; Gill, P. M. W.; Head-Gordon, M.; Pople, J. A. *J. Comput. Chem.* **2000**, *21*, 1532−1548.
(39) Tähtinen, P.; Bagno A.; Klika, K. D.; Pihlaja, K. *J. Am. Chem. Soc.* **2003**, *125*, 4609−4618.
(40) Sheldrick, G. M. *Programs for Crystal Structure Analysis*; Institüt für Anorganische Chemie der Universität, University of Göttingen: Göttingen, Germany, 1998.

NP050004N